ACS Infectious Diseases

Article

Cite This: ACS Infect. Dis. 2019, 5, 851−862

pubs.acs.org/journal/aidcbc

Label-Free Proteomic Analysis Reveals Parasite-Specific Protein Alterations in Macrophages Following *Leishmania amazonensis*, *Leishmania major*, or *Leishmania infantum* Infection

Fernanda Negrão,[*,†,‡,§] Carolina Fernandez-Costa,[†] Nahiara Zorgi,[‡] Selma Giorgio,[‡] Marcos Nogueira Eberlin,[§] and John R. Yates, III[†]

[†]Department of Chemical Physiology, The Scripps Research Institute, 10550 North Torrey Pines Road, SR302, La Jolla, California 92037, United States

[‡]Department of Animal Biology, Institute of Biology, Rua Monteiro Lobato, 255, Campinas, Sao Paulo 13083-862, Brazil

[§]Department of Organic Chemistry, Institute of Chemistry, UNICAMP, Rua Josué de Castro SN, Room A111, Campinas, Sao Paulo 13083-862, Brazil

Supporting Information

ABSTRACT: *Leishmania* is an obligate intracellular parasite known to modulate the host cell to survive and proliferate. However, the complexity of host-parasite interactions remains unclear. Also, the outcome of the disease has been recognized to be *species*-specific and dependent on the host's immune responses. Proteomics has emerged as a powerful tool to investigate the host−pathogen interface, allowing us to deepen our knowledge about infectious diseases. Quantification of the relative amount of proteins in a sample can be achieved using label-free proteomics, and for the first time, we have used it to quantify *Leishmania*-specific protein alterations in macrophages. Protein extracts were obtained and digested, and peptides were identified and quantified using nano-LC coupled with tandem mass spectrometry analyses. Protein expression was validated by Western blot analysis. Integrated Proteomics Pipeline was used for peptide/protein identification and for quantification and data processing. Ingenuity Pathway Analysis was used for network analysis. In this work, we investigated how this intracellular parasite modulates protein expression on a host macrophage by comparing three different Leishmania species—*L. amazonensis*, one of the causative agents of cutaneous disease in the Amazon region; *L. major*, another causative agent of cutaneous leishmaniasis in Africa, the Middle East, China, and India; *L. infantum*, the causative agent of visceral leishmaniasis affecting humans and dogs in Latin America—and lipopolysaccharide stimulated macrophages as an in vitro inflammation model. Our results revealed that Leishmania infection downregulates apoptosis pathways while upregulating the activation of phagocytes/leukocytes and lipid accumulation.

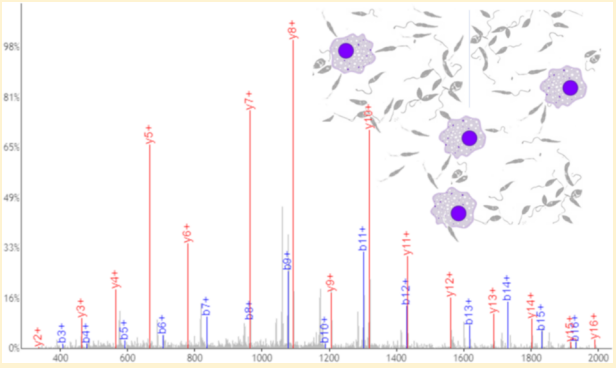

KEYWORDS: *leishmaniasis, host−pathogen interaction, label-free proteomics, mass spectrometry*

Leishmaniasis is an infectious disease caused by an obligate intracellular protozoon of the genus *Leishmania*, which is transmitted through the bite of sandflies. The disease can be caused by more than 20 different *Leishmania* species that result in multiple clinical forms.[1] Leishmaniasis primarily presents as cutaneous, mucocutaneous, or visceral. Estimates of the number of cases of cutaneous and mucocutaneous leishmaniasis per year range from approximately 0.7 million to 1.2 million, while the number of visceral leishmaniasis cases is estimated to range from approximately 0.2 million to 0.4 million per year.[1] *Leishmania* species are morphologically similar, but infection with *Leishmania* can result in different outcomes based on the species and the host's immune responses.[2] It has previously been established that the parasite *Leishmania* reprograms its host cell to meet its metabolic needs,[2] but it is unclear how. Our group has previously demonstrated that *L. infantum* and *L. amazonensis* impact lipid metabolism of host cells differently.[3] In addition, using a murine infection model combining traditional histopathology and Matrix Assisted Laser Desorption Ionization (MALDI) imaging, we have demonstrated that *L. amazonensis* leads to more aggressive infection than *L. major*.[4]

Proteomic approaches have become powerful tools to understand how host−pathogen interactions impact the outcome of infections.[5] This progress was driven by the development of new technologies such as mass spectrometry,

Received: November 29, 2018
Published: April 12, 2019

DOI: 10.1021/acsinfecdis.8b00338
ACS Infect. Dis. 2019, 5, 851−862

which has emerged as a core tool for large-scale protein analysis.[6] Shotgun proteomics is a mass-spectrometry based approach that provides an indirect measurement of proteins through analysis of peptides derived from proteolytic digestion of intact proteins.[6] Using this approach, peptide (and thus, protein) quantification can be achieved through label or label-free techniques. The use of labels is limited by the cost of labeling reagents, inefficient labeling, and difficulty in analysis of low abundance peptides,[6] so we chose to use the straightforward label-free approach for quantification.

In the past decade, the capacity of proteomic analysis has significantly improved through rapid advances in the resolution, mass accuracy, sensitivity, and scan rate of mass spectrometers used to analyze proteins.[7] In addition, increased awareness in the microbiology community has led to the use of these innovative approaches to help understand infectious diseases. Proteomics can be used with molecular biology methods and other "omic" approaches to expand the repertoire of tools available to study infections.[5]

The parasite *Leishmania* has already been studied using proteomics approaches,[8−11] but only a few groups investigated the host−pathogen relationship or compared how infection with different species may lead to different outcomes of the disease.[12,13] Using a J774 macrophage cell line from BALB/c mouse, we compared how three different species (*L. amazonensis*, *L. major*, and *L. infantum*) modulate protein expression in the host. *L. amazonensis*, one of the causative agents of cutaneous leishmaniasis, is usually found only in South America, especially in the Brazilian Amazon region.[14] *L. major* is also a causative agent of cutaneous leishmaniasis, but it is found only in the eastern hemisphere, including northern Africa,[15] the Middle East, northwestern China, and northwestern India.[16] *L. infantum* is one of the causative agents of visceral leishmaniasis which affects humans and dogs and is found in Latin America.[17] Here, we used shotgun proteomics with label-free quantitation to investigate *in vitro* alterations in macrophages following infection with each of these *Leishmania* pathogens.

Previous proteomic analyses to investigate the host response after *Leishmania* infection were reported.[12,18,19] However, this is the first study to compare *Leishmania* infection with an *in vitro* inflammation model (LPS stimulated macrophages) to reveal *Leishmania*-specific protein alterations and to compare the three *Leishmania* species. Proteins were identified and quantified in uninfected; LPS stimulated; and infected macrophages at 24 h post infection (p.i.) with *L. amazonensis*, *L. major*, or *L. infantum*. In addition, biological network analysis was employed to predict altered networks and the respective proteins involved. Our results revealed that apoptotic pathways are inhibited while recruitment of phagocytes/leukocytes and lipid accumulation are enhanced following *Leishmania* infection. We also highlighted proteins that may prove to be interesting targets to deepen our understanding of the infection.

RESULTS AND DISCUSSION

A cascade of specific intracellular interactions that modulate the outcome of an infection is activated when a pathogen meets its host. The understanding of the host−pathogen relationship is crucial for the development of treatments and preventive tools against infectious diseases. Indeed, several transcriptomic reports have already indicated that *Leishmania* modulates host cell metabolism.[20,21] So far, these reports were supported by some proteomic studies.[12,13] Taken together, these data confirm that *Leishmania* masters host cells to ensure parasite survival and proliferation. To date, only a few proteomic studies have evaluated changes in protein expression of host cells following *Leishmania* infection.[12,19,22] Singh and colleagues used an isobaric labeling mass-spectrometry proteomic approach for quantification of proteins that were altered in human macrophages (THP-1 cell line) infected with *L. donovani*.[19] Their results revealed global modulation of host cell metabolism after the infection, such as glycolysis and fatty acid oxidation. Another study reported by Isnard and colleagues used proteomic mass spectrometry as one of the tools to investigate the role of protease GP63, an important virulent factor for *Leishmania spp.* that can potentially subvert host functions for their own benefit. GP63 should be considered for future research as a potential drug target.[19] Veras and colleagues evaluated the protein expression profiles in uninfected CBA macrophages and cells infected with *L. amazonensis* or *L. major* using Multidimensional Protein Identification Technology (MudPIT) analysis, which is characterized by its extensive protein coverage.[23] While MudPIT is typically considered a qualitative proteomics approach, we employed a quantitative analysis using label-free proteomics using an intensity-based approach for quantification, where missing values for peptides can be retrieved after integration of chromatographic peak areas.

In vitro experiments were monitored through microscopy using the Giemsa staining protocol (see Methods section). Infection rate was measured at 12 h, 24 h, and 48 h by counting the number of infected macrophages and the number of amastigotes per macrophage. Experiments were conducted in triplicate. The greatest number of amastigotes per macrophage for *L. amazonensis* and *L. major* was observed at 12 h post infection (p.i.), while all three *Leishmania* species successfully infected J774 macrophages by 24 h (Figure 1) and maintained a persistent infection for at least 72 h.

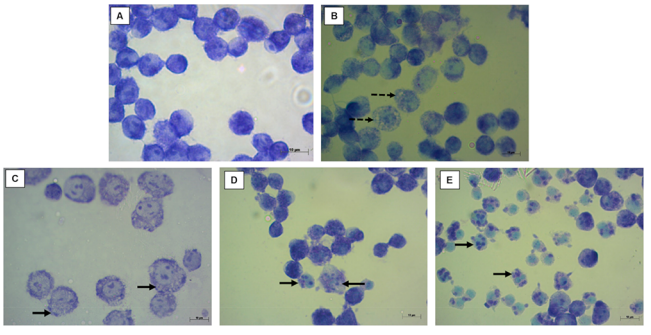

Figure 1. Microscopy of J774 macrophage morphology without infection (A), stimulated with 100 ng/mL of lipopolysaccharide (LPS) for 6 h (B), with infection in the 1:10 macrophage/parasite ratio with *L. amazonesis* (C), *L. major* (D), and *L. infantum* (E) for 24 h and stained with Giemsa. Whole arrows indicate amastigotes in macrophages, and dashed arrows indicate vascularized macrophages. Bar = 10 μm.

The time point of 24 h was chosen to perform label-free quantitative proteomics analysis. At this time, the mean percentage of infected macrophages was 50.6% (±17.39), 48.3% (±3.06), and 59% (±3.61) for *L. amazonensis*, *L. major*, and *L. infantum* infections, respectively. The mean amastigote/

DOI: 10.1021/acsinfecdis.8b00338
ACS Infect. Dis. 2019, 5, 851−862

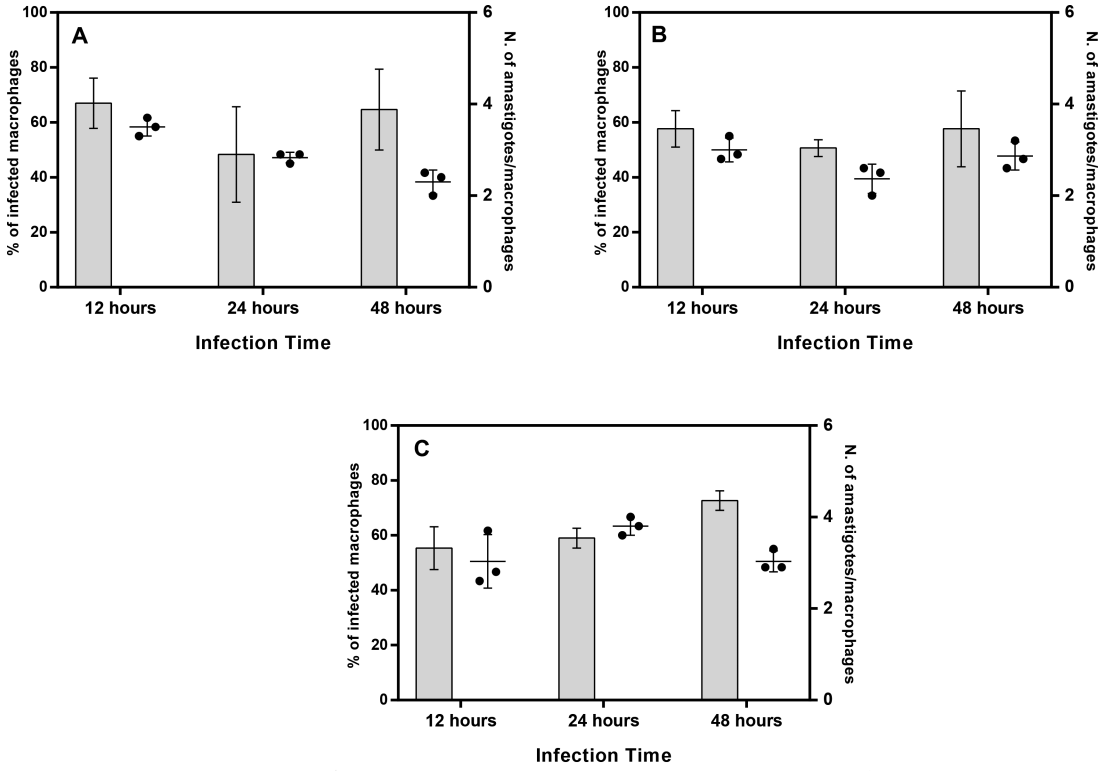

Figure 2. Bars representing the percentage of infected macrophages and dots representing the number of amastigotes per macrophage (amastigote/macrophage ratio) on a three-point time experiment for *L. amazonensis* (A), *L. major* (B), and *L. infantum* (C). The results include data from biological triplicates, and the error bars represent the standard deviations of the means.

macrophage ratio was 2.9 (±0.10), 2.4 (±0.33), and 3.8 (±0.20), respectively (Figure 2).

Modulation of Proteins after *Leishmania* Infection. We performed a label-free quantitative proteomics analysis to search for alterations in protein expression in macrophages following *Leishmania spp.* infection that were compared to an inflammation model (LPS stimulation) to search for *Leishmania*-specific protein modulation. Each condition was composed of five biological replicates. Table S1 shows the total number of proteins that were identified and quantified for each sample, demonstrating the reproducibility of the analysis by means of the number of protein IDs.

To access data reproducibility, we first performed PCA, an unsupervised multivariate method of statistical analysis. Our results showed 77.1% of variance being explained at the first two principal components (Figure S2). The first component reveals that macrophages infected with *L. infantum*, the causative agent of the visceral form of the disease, differ more than macrophages infected with other species and the inflammation model. The second component explains differences observed between healthy macrophages, macrophages infected with *L. amazonensis* or *L. major* (which cause the cutaneous form of the disease), and LPS stimulated macrophages and macrophages infected with *L. major*, which cluster tightly (Figure S2). Heatmaps with hierarchical clustering analysis emphasize that *L. infantum* infected macrophages have greater distance correlation than the other conditions and that healthy macrophages cluster tightly with the inflammation model and with macrophages infected with *L. major* (Figure S3). A mouse model infection had previously revealed that *L. major* infection is less aggressive than the one caused by *L. amazonensis*.[24] This fact could explain the clustering pattern revealed by PCA. Also, PCA and hierarchical clustering were performed to check for differences among infections only (Figures S4, S5). Our results showed that 86.5% of explained variance was at the first two principal components. The first component explains the difference between macrophages infected with *L. infantum* and those infected with *L. amazonensis* or *L. major*. The second component explains the difference between the inflammation model and macrophages infected with *L. amazonensis* or *L. major*. Roughly speaking, the clustering pattern observed from PCA and the heatmap makes biological sense since *L. infantum* is the only investigated species that causes the visceral form of the disease.

The *t* tests were performed as univariate statistical analysis, and fold changes were independently calculated to access changes in protein modulation to provide descriptive information from data sets. Figure S6 displays the volcano plots of proteins significantly modulated (p value < 0.05 and FC ± 1.2) when comparing infections/inflammation versus healthy macrophages. Our results revealed that all protein IDs that were shared between infection and inflammation displayed the same modulation. In other words, most of the proteins that were upregulated after inflammation were also upregulated after infection. Compared with the inflammation model, a total of 266 proteins were exclusively modulated after *L. amazonensis*, 148 after *L. major*, and 209 after *L. infantum* infected macrophages. A Western blot of protein CD9 was performed to validate protein quantification (Figure S1). CD9 (Uniprot ID: P40240) was downregulated after *Leishmania* infection (see Tables S2, S3).

The numbers of altered proteins in healthy macrophages versus infection and versus inflammation are represented in

DOI: 10.1021/acsinfecdis.8b00338
ACS Infect. Dis. 2019, 5, 851−862

Venn diagrams (Figure 3). Protein IDs and their modulations will be discussed in the following sections.

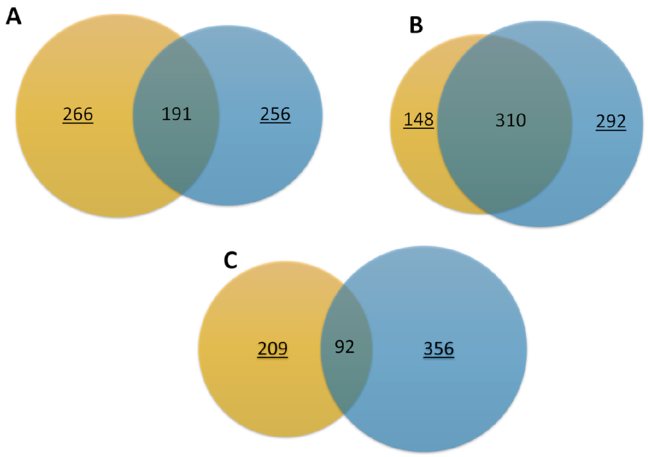

Figure 3. Venn diagrams representing the number of altered proteins comparing healthy macrophages versus infections (in orange) and healthy macrophages versus inflammation (in blue) for the three *Leishmania spp. L. amazonensis* (A): 713 protein IDs (266 + 191 + 256) were statistically significantly modulated compared to healthy and LPS stimulated macrophages; 256 were significantly modulated after inflammation and 266 after infection (211 up- and 55 downregulated). Also, 191 protein IDs were found in common between infection and inflammation, all of which showed the same modulation (i.e., if it was upregulated after inflammation, it was upregulated after infection). *L. major* (B): 750 protein IDs (148 + 310 + 292) were significantly modulated; 148 were specifically modulated after infection (102 were upregulated and 46 were down regulated) and 292 after inflammation. Also, 310 protein IDs were found in common and had shown the same modulation. *L. infantum* (C): 657 proteins (209 + 92 + 356) were significantly modulated following *Leishmania infantum* infection; 209 were specifically modulated after infection (74 were upregulated and 135 were downregulated) and 356 after inflammation. Also, 92 protein IDs were found in common, and they showed the same modulation.

Comparison of Species-Specific Protein Modulation. We have identified proteins that are specifically modulated in macrophages after *Leishmania* infection using label-free quantitative proteomics. Several proteins have never previously been attributed to *Leishmaniasis*, and some confirm previous reports (as will be discussed). We compared macrophage alterations after infection with *Leishmania* species that are known to lead to different outcomes of the disease. First, we compared protein alteration in hosts infected with *L. amazonensis* vs *L. major* and then *L. amazonensis* vs *L. infantum*.

After comparing *L. amazonensis* and *L. major* infection (both causative agents of cutaneous leishmaniasis), a total of 578 proteins were found to be significantly modulated (Table S2). *L. amazonensis* and *L. major* infected macrophages shared a total of 181 protein IDs that had the same modulation (Table S1) such as the upregulation of EF-hand domain-containing protein D2 (EFHD2), synaptosomal-associated protein 23 (SNAP 23), and mitochondrial fission 1 protein (FIS1), which are involved in T cell cytotoxicity,[25] general membrane fusion machinery, and cell signaling, respectively, and the down-regulation of heterogeneous nuclear ribonucleoprotein M (HNRNPM), which is also involved in cell signaling. Only the serine/threonine-protein phosphatase 2A (Ppp2cb; Uniprot ID: P62715; see highlight in Table S2) has shown divergent behavior (upregulated after *L. amazonensis* infection and downregulated after *L. major* infection). An increase in Ppp2cb is known to deactivate MAPK signaling, which is one the major manipulative strategies used by the parasite to cause phagocyte disfunctions.[26] Some of our previous work has demonstrated that infection caused by *L. amazonensis* progresses more aggressively than infection caused by *L. major*,[4,27] which may be explained by the contrasting modulation of this protein. However, the specific role of Ppp2cb in indirectly causing dysfunction of phagocytosis needs to be further investigated.

Besides shared proteins, 396 proteins were found to be differentially regulated in infected macrophages (up- or downregulated after *L. amazonensis* infection and no significant change after *L. major* infection and vice versa). Among these, 275 were modulated after *L. amazonensis* infection and 121 after *L. major* infection. The complete table of protein IDs differentially modulated after *L. amazonensis* or *L. major* infection and their respective fold changes are shown in Table S2.

A comparison of proteins modulated in macrophages after *L. amazonensis* infection versus *L. infantum* showed that a total of 583 proteins were significantly modulated. Among these, 88 proteins were similarly regulated under both conditions (Table S3), including the upregulation of tubulin beta-2A chain (TUBB2A), ubiquitin-60S ribosomal protein L40 (UBA52), polyubiquitin-C and -B (UBC and UBB), and mRNA export factor (RAE1), which are involved in cell signaling, and downregulation of granulins (GRN) and reticulon-3 (RTN3), involved in cell signaling and control of apoptosis, respectively. Also, 494 were found to be differentially regulated (i.e., up- or downregulation after *L. amazonensis* infection and no significant change after *L. infantum* infection and vice versa). Among the 494 differentially regulated proteins, 369 were modulated after *L. amazonensis* infection and 125 after *L. infantum* infection. The complete table of protein IDs and their respective fold changes are shown in Table S4.

Network Analysis of Protein Modulation Following *Leishmania* Infections. Ingenuity Systems Pathway Analysis (IPA-Ingenuity Systems) was used to predict potentially modulated networks following *Leishmania* infection as it facilitates the formulation of new hypotheses from analysis of large data sets, including proteomics.[28] Proteins that were identified as differentially modulated from the comparison of all *Leishmania* infections versus healthy macrophages were used as input to the software IPA-Ingenuity Systems. The highest scored network for each infection was considered to search for protein modulation in other infections, as shown in sections Modulation of Cell Death and Survival Following Leishmania spp. Infection and Modulation of Cell Signaling. For *L. amazonensis* infection, the highest network score was Cell Death and Survival (score 45); for *L. major* infection (score 52) and *L. infantum* (score 53), it was cell signaling. Proteins that are directly correlated to stimulation or inhibition of specific biological events are represented in Figure 4. Our results reveal *Leishmania*-specific alterations in protein expression of host cells, indicating inhibition of cell death and survival pathways, and modulations in cell signaling, including activation of phagocytes/leukocytes and lipid metabolism networks.

Various reports have already confirmed a *Leishmania*-dependent inhibition of host cell apoptosis by several means.[29,30] Our results support previous studies and reveal

DOI: 10.1021/acsinfecdis.8b00338
ACS Infect. Dis. 2019, 5, 851−862

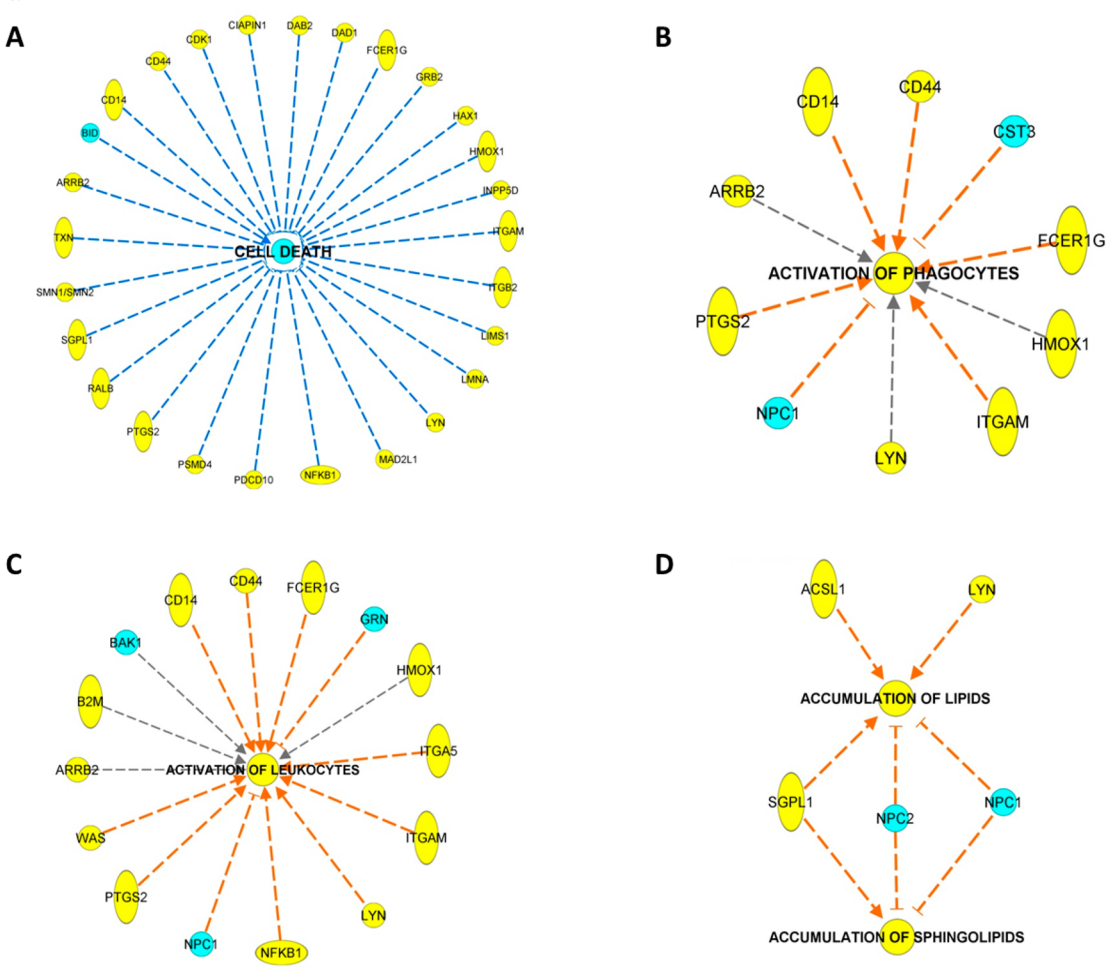

Figure 4. Network analysis for *Leishmania spp.* infected macrophages involving proteins related to cell death (A), activation of phagocytes (B) and leucocytes (C), and accumulation of lipids/sphingolipids (D). Each node represents the expression of a protein present in uninfected macrophages versus pooled information from *Leishmania* infections. Nodes in yellow are upregulated and in blue are downregulated after infection. The networks are colored by their predicted activation state: activated (orange) or inhibited (blue). The edges connecting the nodes are colored yellow when leading to activation of the downstream node and are blue when leading to its inhibition. Networks were built using IPA-Ingenuity Systems.

more proteins that are modulated in the cell death and survival pathways. CD44 antigen (CD44), known as a limiting factor of inflammatory response,[31] heme oxygenase 1 (HMOX), and Ras-related protein Ral-B (RALB) were upregulated in infected macrophages, indicating inhibition of apoptosis. In addition, the downregulation of BH3-interacting domain death agonist (BID) indicates inhibition of cell death (Figure 4A), which is necessary for the infection to persist.[29]

Biological events related to cell-signaling also reveal proteins involved in phagocytosis and immune response (according to IPA output, these events are represented as "activation of phagocytes" and "activation of leukocytes," respectively). As shown in Figure 4B,C, the activation of phagocytes and leukocytes is indicated by the upregulation of CD44, CD14 antigen (CD14), HMOX, beta 2 microglobulin (B2M) and high affinity immunoglobulin gamma Fc receptor I (FCERG1) and by the downregulation of NPC intracellular cholesterol transporter 1 (NPC1) and granulins (GRN). Interestingly, *NPC1* has been reported as an attractive target for the *Ebola* virus as it was identified as a fusion receptor.[32] However, its role in leishmaniasis has to be further investigated.

As being an intracellular microorganism, it is not surprising that after infection *Leishmania* makes changes in the host cell to meet its metabolic needs to survive and replicate within the cell. For instance, the upregulation of genes that encode proteins related to lipid metabolism has been reported[21] and other proteomic findings have supported these transcriptomic reports.[12] Our results deepen the understanding of the pathogenesis of the disease by adding more information on the proteins involved in lipid metabolism. Also, as previously reported,[3,12] leishmaniasis causes disorder in lipid metabolism leading to cell signaling alterations and accumulation of sphingolipids upon infection. Figure 4D represents regulation of proteins that leads to lipid and sphingolipid accumulation by an increase in long-chain-fatty-acid-CoA ligase 1 (ACSL) and tyrosine-protein kinase Lyn (LYN). The most significant protein alterations and their respective fold changes are discussed later. The Acsl gene was previously reported to be upregulated after *L. major* infection,[21] and our results reveal upregulation of protein *acsl* in macrophages infected with *L. amazonensis* and *L. infantum*. Macrophages lacking in the kinase *lyn* are known to have defects in IgG-mediated phagocytosis and amastigote uptake.[33] Our results reveal upregulation of *lyn* in infected macrophages, suggesting that infection could be treated with drugs that inhibit this kinase in host cells. Also, a decrease in NPC1 and 2 along with an

DOI: 10.1021/acsinfecdis.8b00338
ACS Infect. Dis. 2019, 5, 851−862

Table 1. Comparison of Shared Proteins Involved in Cell Death and Survival Pathways after *Leishmania* spp. Infection[a]

gene	Uniprot ID	protein	FC			
			IA[b]	IM[c]	II[d]	LPS[e]
Efhd2	Q9D8Y0	EF-hand domain-containing protein D2	1.77	1.77	1.79	1.84
Fis1	Q9CQ92	mitochondrial fission 1 protein	1.71	1.74	1.77	2.11
Hmox1	P14901	heme oxygenase 1	1.56	1.53	175	1.50
Rtn3	Q9ES97	reticulon-3	1.85	1.66	1.89	–
Dnaja1	P63037	DnaJ homologue subfamily A member 1	1.42	1.34	1.41	1.35
Dab2	P98078	disabled homologue 2	1.53	1.44	1.54	1.46
Bcap31	Q61335	B-cell receptor-associated protein 31	1.50	1.66	1.52	1.55
Ndufa13	Q9ERS2	NADH dehydrogenase	1.60	1.49	1.81	1.61
Cst3	P21460	cystatin-C	0.66	0.64	0.66	0.66
Ralb	Q9JIW9	Ras-related protein Ral-B	1.46	1.55	1.66	1.65
Fcer1g	P20491	high affinity immunoglobulin epsilon receptor subunit gamma	1.35	1.33	1.35	–
Vmp1	Q99KU0	vacuole membrane protein 1	1.44	1.39	1.44	1.46
Nes	Q6P5H2	nestin	1.38	1.53	1.58	1.51
Npc1	O35604	NPC intracellular cholesterol transporter 1	0.75	0.72	0.76	–
Lgals7	O54974	galectin-7	0.66	0.63	0.66	0.64

[a]Blanks (−) are representing nonsignificant fold change (FC) compared to healthy macrophages. [b]IA, *L. amazonensis* infected macrophages. [c]IM, *L. major* infected macrophages. [d]II, *L. infantum* infected macrophages. [e]LPS, lipopolysaccharide stimulated macrophages.

increase in the enzyme sphingosine-1-phosphate lyase 1 indicates accumulation of sphingolipids, which confirms the findings of our previous lipidomics report on *Leishmania* spp.[3]

Modulation of Cell Death and Survival Following *Leishmania* spp. Infection. The cell death and survival network comprised 79 protein IDs, 15 of which were shared among all three infections (Table 1). From these, 12 were upregulated and three were downregulated in macrophages after infection. EF-hand domain-containing protein D2, also known as Swiprosin-1, is acknowledged to play an important role in the macrophage immune response since its depletion decreases survival rates in mice.[25] Our results reveal an increase in Swiprosin-1 after infection, indicating that *Leishmania* might induce the expression of this protein to promote cell survival so the parasite can survive and proliferate. Heme oxygenase 1 (Hmox1) was previously reported to be induced after *L. chagasi* infection and Hmox1 knockout mice presented lower parasite loads, indicating its association with inflammatory imbalance during visceral leishmaniasis.[34] Our results show that *Hmox1* has also increased after infection with the causative agents of cutaneous leishmaniasis (*L. amazonensis* and *L. major*). Our data also reveal a decrease in cystatin-C (CST3), which is known to have a negative regulation in cell death,[35] confirming previous reports on inhibition of apoptosis after leishmania infection.[29]

Moreover, 15 proteins were exclusively modulated after *L. amazonensis* infection, 13 after *L. major*, and another 15 after *L. infantum* infection (Table 2). Note that the "blanks" in the table do not ensure that proteins were not actually present/altered across samples, since our results represent only the proteins that were successfully identified and quantified by mass spectrometry. Phosphatidylinositol 3,4,5-trisphosphate 5-phosphatase 1 (Inpp5d) is known to act as a negative regulator of both B-cell antigen receptor signaling and neutrophil differentiation.[36,37] Our results reveal upregulation of this protein after *L. amazonensis* infection and no significant change after *L. major* or *L. infantum* infection. Other proteins exclusively modulated after *L. amazonensis* infection are mostly related to the apoptotic process, such as the cell division cycle and apoptosis regulator protein 1 (Ccar1) and ubiquitin-conjugating enzyme E2 D3 (Ube2d3), anamorsin (Ciapin1), Bcl-2-like protein 13 (Bcl2l13), and programmed cell death protein 10 (Pdcd10). *Ccar 1* and *Ube2d3* induce apoptosis by activating p53 and caspase-3, respectively,[38,39] and these proteins were downregulated, suggesting inhibition of apoptosis after cells were infected. Additionally, *Ciapin 1* and *Pdcd10* inhibit apoptosis and promote cell proliferation, respectively,[40,41] and these proteins were upregulated in infected macrophages, supporting the previous findings. Conversely, *Bcl2l13*, which is known to activate caspase-3 and therefore induce apoptosis, was upregulated in infected macrophages. This disparate behavior in protein expression needs to be further investigated.

Proteins exclusively modulated after *L. major* infection are also involved in the apoptotic process and cell signaling, including the apoptosis-associated speck-like protein containing a CARD (Pycard), BH3-interacting domain death agonist (Bid), serine/threonine-protein kinase (Pak1), Lyn, nuclear factor NF-kappa-B p105 subunit (Nfkb1), and CD44. Our results revealed downregulation in *Pycard* and *Bid*, both of which induce caspases-mediated apoptosis. Moreover, we observed upregulation of *Pak1*, *Lyn*, *Nfkb11*, and *CD44*. Taken together, these findings suggest inhibition of apoptosis.

Among the proteins exclusively modulated after *L. infantum* infection, mitogen-activated protein kinase 1 (Mapk1) was downregulated. It is known that downregulation of this protein in *L. donovani* parasites is associated with drug resistance;[42] however, its role in infected host cells has not yet been described. Upregulation of integrin alpha-M (Itgam) and downregulation of dynein light chain 1 (Dynll1) and Bcl-2 homologous antagonist/killer (Bak1) also indicates control of apoptosis.

Modulation of Cell Signaling. The cell signaling network comprised 74 protein IDs. Seven proteins were shared among conditions (Table 3) and among these, five were upregulated and two were downregulated after infection. *Fcer1g* and *Hmox1* were previously described as being involved in cell signaling, such as activation of phagocytes and leukocytes. FYN-binding protein 1 (*Fyb1*) is upregulated after all infections, and it is known to play a role in T-cell signaling;[43] its role in leishmaniasis, however, is not known. NPC intracellular cholesterol transporter 1 (*NPC1*) and carnitine O-palmitoyl-

DOI: 10.1021/acsinfecdis.8b00338
ACS Infect. Dis. 2019, 5, 851−862

Table 2. Proteins Exclusively Modulated after *L. amazonensis, L. major,* or *L. infantum* Infection[a]

gene	Uniprot ID	protein	FC			
			IA[b]	IM[c]	II[d]	LPS[e]
Inpp5d	Q9ES52	phosphatidylinositol 3,4,5-trisphosphate 5-phosphatase 1	1.57	–	–	1.48
Vapa	Q9WV55	vesicle-associated membrane protein-associated protein A	1.48	–	–	1.46
Ciapin1	Q8WTY4	anamorsin	1.4	–	–	1.31
Ccar1	Q8CH182	cell division cycle and apoptosis regulator protein 1	0.64	–	–	–
Bcl2l13	P59017	Bcl-2-like protein 13	1.42	–	–	–
Sap18	O55128	histone deacetylase complex subunit SAP18	1.5	–	–	–
Pdcd10	Q8VE70	programmed cell death protein 10	1.72	–	–	–
Chmp4b	Q9D8B3	charged multivesicular body protein 4b	1.24	–	–	–
Sgpl1	Q8R0X7	sphingosine-1-phosphate lyase 1	1.38	–	–	1.48
Naa10	Q9QY36	N-alpha-acetyltransferase 10	1.26	–	–	–
Itgb2	P11835	integrin beta-2 (CD antigen CD18)	1.33	–	–	–
Nme3	Q9WV85	nucleoside diphosphate kinase 3	1.33	–	–	–
Ube2d3	P61079	ubiquitin-conjugating enzyme E2 D3	0.79	–	–	–
Golga2	Q921M4	golgin subfamily A member 2	1.49	–	–	–
Lims1	Q99JW4	LIM and senescent cell antigen-like-containing domain protein 1	–	1.6	–	–
Pqbp1	Q91VJ5	polyglutamine-binding protein 1	–	1.66	–	–
Mrpl41	Q9CQN7	39S ribosomal protein L41, mitochondrial	–	1.5	–	–
Pak1	O88643	serine/threonine-protein kinase PAK 1	–	1.84	–	–
Eif3l	Q8QZY1	eukaryotic translation initiation factor 3 subunit L	–	1.26	–	–
Nfkb1	P25799	nuclear factor NF-kappa-B p105 subunit	–	1.72	–	1.64
Pycard	Q9EPB4	apoptosis-associated speck-like protein containing a CARD	–	0.7	–	0.72
Bid	P70444	BH3-interacting domain death agonist	–	0.69	–	–
Cd44	P15379	CD44 antigen	–	1.32	–	1.37
Lyn	P25911	tyrosine-protein kinase Lyn	–	1.31	–	–
Nup62	Q63850	nuclear pore glycoprotein p62	–	0.71	–	–
Mydgf	Q9CPT4	myeloid-derived growth factor	–	1.3	–	–
Arrb2	Q91YI4	beta-arrestin-2	–	1.36	–	–
Dynll1	P63168	dynein light chain 1, cytoplasmic	–	–	0.64	–
Mapk1	P63085	mitogen-activated protein kinase 1	–	–	0.69	–
Bak1	O08734	Bcl-2 homologous antagonist/killer	–	–	0.67	–
Hk3	Q3TRM8	hexokinase-3	–	–	0.78	–
Nmral1	Q8K2T1	NmrA-like family domain-containing protein 1	–	–	0.7	–
Psmd3	P14685	26S proteasome non-ATPase regulatory subunit 3	–	–	0.78	–
Itgam	P05555	integrin alpha-M (CD11 antigen-like family member B)	–	–	1.4	–
Ogt	Q8CGY8	UDP-N-acetylglucosamine--peptide N-acetylglucosaminyltransferase	–	–	1.38	–
Glmp	Q9JHJ3	glycosylated lysosomal membrane protein	–	–	0.5	–
Fam129b	Q8R1F1	niban-like protein 1	–	–	0.69	–
Spn	P15702	leukosialin (B-cell differentiation antigen LP-3) (CD antigen CD43)	–	–	1.48	–
Smn1	P97801	survival motor neuron protein	–	–	1.41	–
Cops3	O88543	COP9 signalosome complex subunit 3	–	–	0.65	–
Prdx2	Q61171	peroxiredoxin-2	–	–	0.80	–

[a]Blanks (−) are representing nonsignificant fold change (FC) compared to healthy macrophages. [b]IA, *L. amazonensis* infected macrophages. [c]IM, *L. major* infected macrophages. [d]II, *L. infantum* infected macrophages. [e]LPS, lipopolysaccharide stimulated macrophages.

Table 3. Comparison of Common Proteins Modulated after *Leishmania* spp. Infection[a]

gene	Uniprot ID	protein	FC			
			IA[b]	IM[c]	II[d]	LPS[e]
Fyb1	O35601	FYN-binding protein 1	1.5	1.38	1.47	–
Tfrc	Q62351	transferrin receptor protein 1	1.45	1.44	1.46	1.4
Fcer1g	P20491	high affinity immunoglobulin epsilon receptor subunit gamma	1.35	1.33	1	–
Hmox1	P14901	heme oxygenase 1	1.56	1.53	1.75	1.5
Snap23	O09044	synaptosomal-associated protein 23	1.63	1.5	1.52	1.53
Npc1	O35604	NPC intracellular cholesterol transporter 1	0.75	0.72	0.76	–
Cpt2	P52825	carnitine O-palmitoyltransferase 2	0.72	0.7	0.69	0.77

[a]Blanks (−) are representing nonsignificant fold change (FC) compared to healthy macrophages. [b]IA, *L. amazonensis* infected macrophages. [c]IM, *L. major* infected macrophages. [d]II, *L. infantum* infected macrophages. [e]LPS, lipopolysaccharide stimulated macrophages.

DOI: 10.1021/acsinfecdis.8b00338
ACS Infect. Dis. 2019, 5, 851−862

Table 4. Proteins Exclusively Modulated after *L. amazonensis*, *L. major*, or *L. infantum* Infection[a]

gene	Uniprot ID	protein	FC			
			IA[b]	IM[c]	II[d]	LPS[e]
Txnrd2	Q9JLT4	thioredoxin reductase 2	1.5	–	–	–
Inpp5d	Q9ES52	phosphatidylinositol 3,4,5-trisphosphate 5-phosphatase 1	1.57	–	–	1.48
Was	P70315	Wiskott–Aldrich syndrome protein homologue (WASp)	1.61	–	–	1.53
Zc3hav1	Q3UPF5	zinc finger CCCH-type antiviral protein 1	1.36	–	–	–
Tbcb	Q9D1E6	tubulin-folding cofactor B	1.66	–	–	1.75
Rpl10a	P53026	60S ribosomal protein L10a	1.2	–	–	–
Ciapin1	Q8WTY4	anamorsin	1.39	–	–	1.31
B2m	P01887	beta-2-microglobulin	1.43	–	–	–
Itgb2	P11835	integrin beta-2 (CD antigen CD18)	1.32	–	–	–
Ptges2	Q8BWM0	prostaglandin E synthase 2	1.41	–	–	–
Hcfc1	Q61191	host cell factor 1 (HCF) (HCF-1) (C1 factor)	1.38	–	–	–
Jagn1	Q5XKN4	protein jagunal homologue 1	1.4	–	–	–
Ube2d2	P62838	ubiquitin-conjugating enzyme E2 D2	0.79	–	–	–
Sgpl1	Q8R0X7	sphingosine-1-phosphate lyase 1	1.38	–	–	–
Npc2	Q9Z0J0	NPC intracellular cholesterol transporter 2	0.74	–	–	–
Acp6	Q8BP40	lysophosphatidic acid phosphatase type 6	0.74	–	–	–
Hdlbp	Q8VDJ3	vigilin (high density lipoprotein-binding protein; HDL-binding protein)	1.39	–	–	–
Lyn	P25911	tyrosine-protein kinase Lyn	–	1.31	–	–
Pfkp	Q9WUA3	ATP-dependent 6-phosphofructokinase, platelet type	–	1.36	–	1.31
Ppp2ca	P63330	serine/threonine-protein phosphatase 2A catalytic subunit alpha isoform	–	1.2	–	1.21
Nfkb1	P25799	nuclear factor NF-kappa-B p105 subunit	–	1.71	–	1.64
Ppp1r11	Q8K1L5	E3 ubiquitin-protein ligase PPP1R11	–	1.65	–	–
Arrb2	Q91YI4	beta-arrestin-2 (Arrestin beta-2)	–	1.36	–	–
Cd44	P15379	CD44 antigen	–	1.31	–	1.37
Pycard Asc	Q9EPB4	apoptosis-associated speck-like protein containing a CARD	–	0.7	–	0.72
Itga5	P11688	integrin alpha-5 (CD49 antigen-like family member E)	–	1.53	–	
Nup98	Q6PFD9	nuclear pore complex protein Nup98-Nup96	–	1.44	–	–
Pqbp1	Q91VJ5	polyglutamine-binding protein 1	–	1.65	–	–
ABL78_8321	A0A0N1HR67	tubulin alpha chain	–	1.7	–	–
Mapk1	P63085	mitogen-activated protein kinase 1	–	–	0.69	–
Spn	P15702	leukosialin	–	–	1.47	–
Pafah1b	P63005	platelet-activating factor acetylhydrolase IB subunit alpha	–	–	0.7	–
Fabp5	Q05816	fatty acid-binding protein 5	–	–	0.73	–
Itgam	P05555	integrin alpha-M	–	–	1.39	–
Cd180	Q62192	CD180 antigen	–	–	0.68	–
Pum2	Q80U58	pumilio homologue 2	–	–	2.42	–
Bak1 Bak	O08734	Bcl-2 homologous antagonist/killer	–	–	0.67	–
Ube2i	P63280	SUMO-conjugating enzyme UBC9	–	–	0.75	–
Ube2d2b	Q6ZWY6	ubiquitin-conjugating enzyme E2 D2B	–	–	1.62	–
Acadvl	P50544	very long-chain specific acyl-CoA dehydrogenase, mitochondrial	–	–	1.38	–
Hadhb	Q99JY0	trifunctional enzyme subunit beta, mitochondrial	–	–	0.74	–
Lta4h	P24527	leukotriene A-4 hydrolase	–	–	0.75	–

[a]Blanks (−) are representing nonsignificant fold change (FC) compared to healthy macrophages. [b]IA, *L. amazonensis* infected macrophages. [c]IM, *L. major* infected macrophages. [d]II, *L. infantum* infected macrophages. [e]LPS, lipopolysaccharide stimulated macrophages.

transferase 2 (*Cpt2*) are downregulated after all infections, indicating alterations in lipid metabolism. It has already been described that reduction of *NPC1*, a protein that is responsible for cholesterol efflux from endocytic compartments, causes accumulation of cholesterol in infected macrophages and ultimately leads to an impairment in immune signaling functions. However, this outcome seems to depend on the number of intracellular amastigotes. *NPC1* could be an interesting target in host cells to impair parasite survival.

Moreover, 18 proteins were exclusively modulated after *L. amazonensis* infection, 12 after *L. major*, and another 13 after *L. infantum* infection (Table 4). Among proteins exclusively altered in macrophages after *L. amazonensis* infection, there was an increase in prostaglandin E synthase 2 (*Ptges2*) and *Sgpl1*; elongation of very long chain fatty acids protein 1 (*Elovl1*), lysophosphatidic acid phosphatase type 6 (*Acp6*), and Vigilin (*Hdlbp*); and a decrease in *NPC2*, indicating accumulation of lipids/disorder in lipid metabolism. Our results also reveal upregulation of previously mentioned proteins *Ciapin1* and *Inpp5d* in *L. amazonensis* infected macrophages, suggesting stimulation of cytokine and growth factors that favor parasite proliferation. It is known that elevation in *Inpp5d* can lead to negative modulation of neutrophil recruitment and modulate defense responses in the host.[37] Activation of neutrophils is necessary to clear the infection to some species of *Leishmania*, including *L. amazonensis*.[37] As any other host target, this phosphatase has

DOI: 10.1021/acsinfecdis.8b00338
ACS Infect. Dis. 2019, 5, 851−862

to be carefully investigated as a drug target due to its possible side effects.

Proteins exclusively modulated in macrophages after *L. major* infection primarily reveal upregulation of proteins involved in cell signaling processes and downregulation of *Pycard*, a protein already mentioned to be associated with induction of apoptosis.

Proteins exclusively modulated in macrophages after *L. infantum* infection are mostly downregulated, including *Mapk1*, platelet-activating factor acetylhydrolase IB subunit alpha (*Pafah1b*), fatty acid-binding protein 5 (*Fabp5*), CD180 antigen (*CD180*), and *Bak1*.

CONCLUSIONS

In summary, we have demonstrated how the parasite *Leishmania* modulates protein expression in infected macrophages differently than in an inflammation model, including identification of exclusively modulated proteins after *Leishmania* exposure. However, all proteins shared between infections and inflammation showed the same modulation. Moreover, we revealed a species-specific modulation of proteins that has not previously been ascribed to leishmaniasis.

Among protein IDs that were shared between *L. amazonensis* versus *L. major* infected macrophages, only *Ppp2cb* showed opposite modulation. Moreover, 275 proteins were exclusively modulated in macrophages after *L. amazonensis* and 121 after *L. major* infection. When comparing *L. amazonensis* versus *L. infantum* infected macrophages, 269 proteins were exclusively modulated following *L. amazonensis* infection, whereas 125 were modulated following *L. infantum* infection.

The quantification of 79 proteins involved in cell death and 74 proteins involved in cell signaling networks suggests inhibition of apoptosis and activation of phagocytes/leukocytes and accumulation of lipids/sphingolipids.

Interestingly, the phosphatase *Inpp5d* was upregulated after *L. amazonensis* infection, which might lead to a deficit in recruitment of neutrophils leading to parasite persistance, especially when compared to *L. major* infection. This phosphatase would be an interesting target to investigate host response against *L. amazonensis* infection. Downregulation of the kinase *Mapk1* was observed in macrophages following *L. infantum* infection. Moreover, upregulation of *Ppp2cb* in *L. amazonensis* infected macrophages also leads to deactivation of *Mapk* signaling, suggesting this kinase could be a potential drug target against leishmaniasis. Also, the role of *NPC1* should be further investigated for leishmaniasis since it has been reported as an attractive target for intracellular microorganisms, and it was downregulated after *Leishmania* spp. infections.

Our findings raise interesting questions about how different species of *Leishmania* modulate protein expression in infected macrophages, so we can deepen the understanding of how *Leishmania* modulates host cells to establish the infection. Further investigations of modulated proteins in macrophages after exposure to *Leishmania* parasites could identify potential targets to control the disease, such as immunotherapy, or to restore the metabolism of macrophages.

METHODS

Parasite Culture. *L. amazonensis*, strain MHOM/BR/67/M2269; *L. major*, strain *Friedlin*; and *L. infantum*, strain MHOM/BR/1972/LD were maintained by regular passage in BALB/c mice, in accordance with Ethics Committee number 4041-1 (CEUA/UNICAMP Universidade Estadual de Campinas). *L. amazonensis* and *L. major* promastigotes were kept in RPMI medium containing 10% FBS and gentamicin at 50 μg/mL at pH 7.4. *L. infantum* promastigotes were grown in Schneider medium supplemented with 10% fetal bovine serum (FBS, from SIGMA), 5% filtrated urine, and gentamicin at 50 μg/mL. Parasite cultures were maintained at 26°C.

***J774* Macrophage Infection and Microscopic Assay.** The *J774* macrophage cell line from BALB/c mice was obtained from the American Type Culture Collection. Cells were grown at 37 °C in RPMI medium supplemented with 10% FBS and 50 μg/mL of gentamicin in a humidified atmosphere of 5% CO_2. A total of 5 $\times 10^6$ cells were plated in six-well plates and maintained for 18 h. Promastigotes were then added to macrophages at a ratio of 10:1 parasites/cell. *Escherichia coli* lipopolysaccharide (LPS; Sigma) stimulated macrophages were used as an inflammation model by adding 100 ng/μL of LPS to each well for 24 h.[44] *In vitro* assays were conducted in five replicates for each condition (healthy, LPS-stimulated and -infected macrophages). After infection, the J774 macrophages were fixed with methanol (Synth 99,8%) for 10 min and stained by Giemsa (Fluka analytical) in buffer (1/20 ratio of potassium phosphate monobasic KH_2PO_4 0.07 and 0.07 M bibasic sodium phosphate Na_2HPO_4) for 3 min. Using a microscope at 100× magnification, the percentage of infected macrophages and the amastigote/macrophage ratio were determined. At least 100 adhered macrophages and the number of amastigotes were counted, as previously described.[45] The percentage of infected macrophages was calculated by counting up to 100 macrophages and dividing the total number of infected macrophages by 100. The amastigote/macrophage ratio was determined by dividing the total number of infected macrophages by the total number of amastigotes. The experiment was performed in biological triplicates, and the counting/calculations were performed two times independently. The respective standard deviations of the means were calculated and plotted in graphs.

Protein Extraction and Digestion Protocol. After incubation, cells were kept on ice and scraped off plate wells, and protein extraction was performed in 300 μL of lysis buffer (7 M urea, 2 M thiourea, 40 mM Tris and 2% CHAPS), supplemented with PMSF as a protease inhibitor. All reagents were from Sigma-Aldrich. The solutions were homogenized for 30 min and centrifuged at 13 800*g* for 20 min at 4 °C. Proteins were precipitated by adding a mixture of chloroform/methanol/water (3:4:1) and homogenizing for 5 min followed by centrifugation at 13 800*g* for 10 min. The intermediate phase, which is the precipitate, was carefully separated from the upper and bottom phases with a pipet. To obtain a pellet, precipitates were centrifuged at 12 000*g* after adding 200 μL of methanol. The upper phase was removed, and the pellet was allowed to dry.

Samples were resuspended in 100 mM TEAB buffer, and protein concentration was determined using a Pierce BCA Protein Assay Kit from Thermo Scientific. A total of 100 μg of protein per sample was used for digestion. Solubilized proteins were reduced by adding TCEP to 5 mM as a final concentration, alkylated by adding chloroacetamide to a 55 mM final concentration and left for 15 min in the dark at room temperature. Next, calcium chloride was added to a 1 mM final concentration. Finally, proteins were digested by incubating with 1:50 (enzyme/protein, w/w) trypsin overnight at 37 °C

DOI: 10.1021/acsinfecdis.8b00338
ACS Infect. Dis. 2019, 5, 851−862

with vigorous orbital shaking. Digestion was interrupted by adding 90% trifluoroacetic acid solution to 5% final concentration.

Data Acquisition. Peptides were analyzed by nano LC-MS/MS coupled to an LTQ-Orbitrap Velos mass spectrometer (Thermo Fisher Scientific, Bremen, Germany). Samples were randomly injected using an autosampler and eluted on a column self-packed with C18 reversed-phase resin (Phenomenex, 100 μm inner diameter × 3 μm × 20 mm) using a 1 to 80% gradient of solvent B (acetonitrile) over 120 min at a 400 nL/min flow rate. Blanks were injected between samples to avoid carry-over effects. The LTQ-Orbitrap Velos was operated in data-dependent acquisition mode with the XCalibur software. Survey scan mass spectra were acquired in the Orbitrap on the 400−2000 m/z range with the resolution set to 60 000 (fwhm). The 10 most intense ions per survey scan were selected for CID fragmentation, and the resulting fragments were analyzed in the linear trap (LTQ). Dynamic exclusion was employed within 120 s to prevent repetitive selection of the same peptide.

Protein Identification, Quantification, and Normalization. Raw files were extracted into ms1 and ms2 files from raw files using Raw Converter 1.1.0.19 (http://fields.scripps.edu/rawconv/). Protein identification was performed using the Integrated Proteomics Pipeline-IP2 (Integrated Proteomics Applications; http://www.integratedproteomics.com/). Using a minimum length of six amino acids, mass spectra were searched for peptide identifications with ProLuCID.[46] ProLuCID results were filtered using DTASelect2[47] to a false discovery rate (FDR) at the protein level of 1%. All tandem mass spectrometry (MS/MS) spectra were compared using the search algorithm ProLuCID[46] against theoretical mass spectra calculated from the *in silico* digested reference database (UniprotKB/*Mus musculus* (mouse) release 2018_04) using a decoy strategy.[48] Precursor mass tolerance was set to 50 ppm and fragment ion tolerance to 600 ppm for CID spectra with carbamidomethylation of cysteine as a static modification. The FDR was calculated based on the number of PSMs that matched sequences in the reverse decoy database of *Mus musculus*.

Census[49] was employed for quantification of proteins and performed at the MS1 level using an intensity based approach that involves integration of chromatographic peak areas of all the peptides of a given protein. Peptides were evaluated after first searching with ProLuCID and a peptide need only be identified in one of the replicates to be quantified (missing values were retrieved in the aligned chromatogram). MS1 scans were used by Census for chromatogram reconstruction and alignment using dynamic time warping.[49] Thus, the process for quantification of proteins is based on *area under the curve* (AUC) by measurement of ion abundance at specific retention times for given ionized peptides. Protein abundances were normalized by the sum of all peptides measured for a given sample, and log base 2 transformation was applied.

Statistical Analysis. Five biological replicates were measured for each biological condition (healthy macrophage, *L. amazonensis*/*L. major*/*L. infantum* infected macrophages, and LPS stimulated macrophages). Normalized data were accessed by principal component analysis (PCA), an unsupervised multivariate statistical analysis to check for data reproducibility and sample preparation using the online server MetaboAnalyst 4.0 (www.metaboanalyst.ca).[50] Then, a univariate analysis using t test and fold change calculations were performed to evaluate changes in protein abundance independently to provide descriptive information from infections versus inflammation. Fold change was determined by the ratio group x/group y, where "group x" is the average of normalized intensity for condition x and "group y" is the average of normalized intensity for healthy macrophage. p values were calculated to assess changes in protein expression in macrophages after different stimulations (*Leishmania* spp. or LPS). P values were individually calculated by comparing two conditions at a time (healthy macrophage versus infection; healthy macrophage versus inflammation). P values were corrected using the Benjamini−Hochberg procedure.[51] First, each individual p value was ranked from smallest to largest (from 1 to n); then the correction was calculated by the equation: $(i/m) \times Q$, where i is the rank, m is the total number of tests, and Q is the false discovery rate that was set as 5% (0.05). The largest p value that had $P < (i/m) \times Q$ was considered significant, and all of the P values smaller than it are also significant. Corrected p values < 0.05 were considered as statistically significant. Correlation between p values and FC were represented by volcano plots. Next, heatmaps with Ward's hierarchical clustering method using the most statistically modulated proteins were assessed to further the visualization of data sets.

Validation of Protein Quantification Using Western Blot Analysis. The extracts of uninfected macrophages (MØ) or cells infected with *L. amazonensis* (L.a.) or LPS stimulation were obtained after 24 h of incubation. CD9 antigen was selected for validation since it showed opposite modulation in infection versus inflammation. CD9 was downregulated in infected macrophages and upregulated in LPS stimulated macrophages. A total of 20 μg of lysate from each condition was loaded onto a Bolt 4−12% Bis-Tris Plus Gel (Thermo Scientific) and transferred to a nitrocellulose membrane (Thermo Scientific). The proteins were immunostained using anti-CD9 antigen (sc-13118, Santa Cruz Biotechnology) diluted 1:500 with blocking buffer (5% nonfat dry milk in Tris buffered saline with Tween 20 (Sigma-Aldrich)), followed by incubation with the secondary antibody (HRP, Thermo Scientific) diluted 1:5000 with blocking buffer. Sequentially, anti-GAPDH (ab181602, Abcam) diluted 1:1000 with blocking buffer was used as a loading control followed by incubation with a secondary antibody antirabbit HRP (ab205718, Abcam) diluted 1:5000 with blocking buffer. An ECL Western Blotting kit (#32106, Thermo Scientific) was used as the chemiluminescence reagent. Western blot images were acquired on a scanner station and analyzed for mean intensity above the background. Fold change was determined by densitometry (triplicate) using ImageJ.[52] Statistical analysis was performed using a Mann−Whitney U Test.

IPA Network Analysis. Ingenuity Systems Pathway Analysis v8.8 software (IPA-Ingenuity Systems, Redwood City, CA, USA) was used to predict networks that involve the selected proteins under different conditions (healthy, LPS stimulated, and infected macrophages). The potential networks were scored and modeled considering protein identities (IDs) that revealed a p value lower than <0.05 and a fold change of ±1.2 after protein quantification.

DOI: 10.1021/acsinfecdis.8b00338
ACS Infect. Dis. 2019, 5, 851−862

■ ASSOCIATED CONTENT

Supporting Information

The Supporting Information is available free of charge on the ACS Publications website at DOI: 10.1021/acsinfecdis.8b00338.

Table S1, total number of protein identities for each sample; Table S2, list of shared proteins between *L. amazonensis* and *L. major* infection and their fold changes; Table S3, list of shared proteins between *L. amazonensis* and *L. infantum* infection and their fold changes; Table S4, list of differentially modulated proteins in macrophages after *L. amazonensis* or *L. major* infection; Table S5, list of differentially modulated proteins in macrophages after *L. amazonensis* or *L. infantum* infection; Figure S1, Western Blotting validation in CD9 expression; Figure S2, assessment of data quality using PCA for the complete data set); Figure S3, heatmap/hierarchical clustering for the complete data set; Figure S4, assessment of data quality using PCA for infections; Figure S5, heatmap/hierarchical clustering for infections; Figure S6, volcano plots (PDF)

Normalized abundance of all identified proteins across samples; fold changes; original and corrected p-values (FDR) for each comparison (XLSX)

■ AUTHOR INFORMATION

Corresponding Author

*E-mail: negraosf@gmail.com.

ORCID

Fernanda Negrão: 0000-0002-9839-6511

John R. Yates, III: 0000-0001-5267-1672

Notes

The authors declare no competing financial interest.

■ ACKNOWLEDGMENTS

F.N. acknowledges FAPESP (2017/22651-4), C.F.C. for contributing with mass spectrometry data acquisition, and N.Z. for microscopic assays. S.G. acknowledges FAPESP 2015/23767-0, and J.Y. acknowledges P41 GM103533.

■ REFERENCES

(1) CDC - Leishmaniasis - Biology. https://www.cdc.gov/parasites/leishmaniasis/biology.html (published 2017; accessed September 17, 2018).

(2) Rossi, M., and Fasel, N. (2018) How to master the host immune system? Leishmania parasites have the solutions! *Int. Immunol. 30* (3), 103−111.

(3) Negrão, F., Abánades, D. R., Jaeeger, C. F., et al. (2017) Lipidomic alterations of in vitro macrophage infection by L. infantum and L. amazonensis. *Mol. BioSyst. 13* (11), 2401−2406.

(4) Negrão, F., de O. Rocha, D. F., Jaeeger, C. F., Rocha, F. J. S., Eberlin, M. N., and Giorgio, S. (2017) Murine cutaneous leishmaniasis investigated by MALDI mass spectrometry imaging. *Mol. BioSyst. 13* (10), 2036−2043.

(5) Jean Beltran, P. M., Federspiel, J. D., Sheng, X., and Cristea, I. M. (2017) Proteomics and integrative omic approaches for understanding host-pathogen interactions and infectious diseases. *Mol. Syst. Biol. 13* (3), 922.

(6) Zhang, Y., Fonslow, B. R., Shan, B., Baek, M., and Yates, J. R. (2013) Protein Analysis by Shotgun/Bottom-up Proteomics. *Chem. Rev. 113* (4), 2343−2394.

(7) Makarov, A., Denisov, E., Kholomeev, A., et al. (2006) Performance Evaluation of a Hybrid Linear Ion Trap/Orbitrap Mass Spectrometer. *Anal. Chem. 78*, 2113−2120.

(8) Veras, P., and Bezerra de Menezes, J. (2016) Using Proteomics to Understand How Leishmania Parasites Survive inside the Host and Establish Infection. *Int. J. Mol. Sci. 17*, 1270.

(9) Lynn, M. A., Marr, A. K., and McMaster, W. R. (2013) Differential quantitative proteomic profiling of Leishmania infantum and Leishmania mexicana density gradient separated membranous fractions. *J. Proteomics 82*, 179−192.

(10) Wright, M. H., Paape, D., Storck, E. M., Serwa, R. A., Smith, D. F., and Tate, E. W. (2015) Global analysis of protein N-myristoylation and exploration of N-myristoyltransferase as a drug target in the neglected human pathogen Leishmania donovani. *Chem. Biol. 22* (3), 342−354.

(11) Walker, J., Vasquez, J. J., Gomez, M. A., et al. (2006) Identification of developmentally-regulated proteins in Leishmania panamensis by proteome profiling of promastigotes and axenic amastigotes. *Mol. Biochem. Parasitol. 147* (1), 64−73.

(12) Menezes, J. P. B., Almeida, T. F., Petersen, A. L. O. A., et al. (2013) Proteomic analysis reveals differentially expressed proteins in macrophages infected with Leishmania amazonensis or Leishmania major. *Microbes Infect. 15* (8−9), 579−591.

(13) da Silva Santos, C., Attarha, S., Saini, R. K., et al. (2015) Proteome profiling of human cutaneous leishmaniasis lesion. *J. Invest. Dermatol. 135* (2), 400−410.

(14) Reithinger, R., Dujardin, J.-C., Louzir, H., Pirmez, C., Alexander, B., and Brooker, S. (2007) Review Cutaneous leishmaniasis. *Lancet Infect. Dis. 7*, 581.

(15) Aoun, K., and Bouratbine, A. (2014) Cutaneous leishmaniasis in North Africa: a review. *Parasite 21*, 14.

(16) Inbar, E., Akopyants, N. S., Charmoy, M., et al. (2013) The mating competence of geographically diverse Leishmania major strains in their natural and unnatural sand fly vectors. *PLoS Genet. 9* (7), No. e1003672.

(17) El Hajj, R., El Hajj, H., and Khalifeh, I. (2018) Fatal Visceral Leishmaniasis Caused by Leishmania infantum, Lebanon. *Emerging Infect. Dis. 24*, 906.

(18) Isnard, A., Christian, J. G., Kodiha, M., Stochaj, U., McMaster, W. R., Olivier, M., and Müller, I. (2015) Impact of Leishmania Infection on Host Macrophage Nuclear Physiology and Nucleopore Complex Integrity. *PLoS Pathog. 11* (3), No. e1004776.

(19) Singh, A. K., Pandey, R. K., Siqueira-Neto, J. L., et al. (2015) Proteomic-based approach to gain insight into reprogramming of THP-1 cells exposed to Leishmania donovani over an early temporal window. *Infect. Immun. 83* (5), 1853−1868.

(20) Beattie, L., D'El-Rei Hermida, M., Moore, J. W. J., et al. (2013) A transcriptomic network identified in uninfected macrophages responding to inflammation controls intracellular pathogen survival. *Cell Host Microbe 14* (3), 357−368.

(21) Rabhi, I., Rabhi, S., and Ben-Othman, R. (2012) Transcriptomic Signature of Leishmania Infected Mice Macrophages: A Metabolic Point of View. *PLoS Neglected Trop. Dis. 6* (8), e1763.

(22) Isnard, A., Christian, J. G., Kodiha, M., Stochaj, U., McMaster, W. R., and Olivier, M. (2015) Impact of Leishmania infection on host macrophage nuclear physiology and nucleopore complex integrity. *PLoS Pathog. 11* (3), No. e1004776.

(23) Schirmer, E. C., Yates, J. R., and Gerace, L. (2003) MudPIT: A powerful proteomics tool for discovery. *Discov Med. 3* (18), 38−39.

(24) Negrão, F., de O. Rocha, D. F., Jaeeger, C. F., Rocha, F. J. S., Eberlin, M. N., and Giorgio, S. (2017) Murine cutaneous leishmaniasis investigated by MALDI mass spectrometry imaging. *Mol. BioSyst. 13* (10), 2036.

(25) Zhang, S., Tu, Y., and Sun, Y.-M. (2018) Swiprosin-1 deficiency impairs macrophage immune response of septic mice. *JCI Insight 3* (3), e95396 DOI: 10.1172/jci.insight.95396.

(26) Kar, S., Ukil, A., Sharma, G., and Das, P. K. (2010) MAPK-directed phosphatases preferentially regulate pro- and anti-inflamma-

tory cytokines in experimental visceral leishmaniasis: involvement of distinct protein kinase C isoforms. *J. Leukocyte Biol. 88* (1), 9−20.
(27) Scorza, B., Carvalho, E., and Wilson, M. (2017) Cutaneous Manifestations of Human and Murine Leishmaniasis. *Int. J. Mol. Sci. 18* (6), 1296.
(28) Krämer, A., Green, J., Pollard, J., and Tugendreich, S. (2014) Causal analysis approaches in Ingenuity Pathway Analysis. *Bioinformatics 30* (4), 523−530.
(29) Moore, K. J., and Matlashewski, G. (1994) Intracellular infection by Leishmania donovani inhibits macrophage apoptosis. *J. Immunol 152* (6), 2930−2937.
(30) Pandey, R. K., Mehrotra, S., Sharma, S., Gudde, R. S., Sundar, S., and Shaha, C. (2016) Leishmania donovani-Induced Increase in Macrophage Bcl-2 Favors Parasite Survival. *Front. Immunol. 7*, 456.
(31) Johnson, P., and Ruffell, B. (2009) CD44 and its role in inflammation and inflammatory diseases. *Inflammation Allergy: Drug Targets 8* (3), 208−220.
(32) Kuroda, M., Fujikura, D., Nanbo, A., et al. (2015) Interaction between TIM-1 and NPC1 Is Important for Cellular Entry of Ebola Virus. *J. Virol. 89* (12), 6481−6493.
(33) Wetzel, D. M., Rhodes, E. L., Li, S., McMahon-Pratt, D., and Koleske, A. J. (2016) The Src kinases Hck, Fgr and Lyn activate Arg to facilitate IgG-mediated phagocytosis and Leishmania infection. *J. Cell Sci. 129* (16), 3130.
(34) Luz, N. F., Andrade, B. B., Feijó, D. F., et al. (2012) Heme oxygenase-1 promotes the persistence of Leishmania chagasi infection. *J. Immunol. 188* (9), 4460−4467.
(35) Cst3 - Cystatin-C precursor - Mus musculus (Mouse) - Cst3 gene & protein. https://www.uniprot.org/uniprot/P21460 (accessed October 2, 2018).
(36) Nishio, M., Watanabe, K., Sasaki, J., et al. (2007) Control of cell polarity and motility by the PtdIns(3,4,5)P3 phosphatase SHIP1. *Nat. Cell Biol. 9* (1), 36−44.
(37) Luo, H. R., and Mondal, S. (2015) Molecular control of PtdIns(3,4,5)P3 signaling in neutrophils. *EMBO Rep. 16* (2), 149.
(38) Uniprot.ccar1 in UniProtKB. https://www.uniprot.org/uniprot/?query=CCAR1&sort=score (accessed October 4, 2018).
(39) Uniprot.ube2d3 in UniProtKB. https://www.uniprot.org/uniprot/?query=Ube2d3&sort=score (accessed October 4, 2018).
(40) Shibayama, H., Takai, E., Matsumura, I., et al. (2004) Identification of a Cytokine-induced Antiapoptotic Molecule Anamorsin Essential for Definitive Hematopoiesis. *J. Exp. Med. 199* (4), 581−592.
(41) He, Y., Zhang, H., Yu, L., et al. (2010) Stabilization of VEGFR2 Signaling by Cerebral Cavernous Malformation 3 Is Critical for Vascular Development. *Sci. Signaling 3* (116), ra26−ra26.
(42) Ashutosh, Garg, M., Sundar, S., Duncan, R., Nakhasi, H. L., and Goyal, N. (2012) Downregulation of mitogen-activated protein kinase 1 of Leishmania donovani field isolates is associated with antimony resistance. *Antimicrob. Agents Chemother. 56* (1), 518−525.
(43) da Silva, A. J., Li, Z., de Vera, C., Canto, E., Findell, P., and Rudd, C. E. (1997) Cloning of a novel T-cell protein FYB that binds FYN and SH2-domain-containing leukocyte protein 76 and modulates interleukin 2 production. *Proc. Natl. Acad. Sci. U. S. A. 94* (14), 7493−7498.
(44) Mosser, D. M., and Zhang, X. (2008) Activation of murine macrophages. *Curr. Protoc Immunol 83*, 14.2.1−14.2.8, DOI: 10.1002/0471142735.im1402s83.
(45) Terreros, M. J. S., de Luna, L. A. V., and Giorgio, S. (2017) Long-term cell culture isolated from lesions of mice infected with Leishmania amazonensis: a new approach to study mononuclear phagocyte subpopulations during the infection. *Pathog. Dis. 75* (8), ftx114 DOI: 10.1093/femspd/ftx114.
(46) Eng, J. K., McCormack, A. L., and Yates, J. R. (1994) An approach to correlate tandem mass spectral data of peptides with amino acid sequences in a protein database. *J. Am. Soc. Mass Spectrom. 5* (11), 976−989.
(47) Cociorva, D., Tabb, L. D., and Yates, J. R. (2007) Validation of Tandem Mass Spectrometry Database Search Results Using DTASelect, in *Current Protocols in Bioinformatics*, Chapter 13, Unit 13.4, John Wiley & Sons, Inc., Hoboken, NJ, DOI: 10.1002/0471250953.bi1304s16.
(48) Elias, J. E., and Gygi, S. P. (2007) Target-decoy search strategy for increased confidence in large-scale protein identifications by mass spectrometry. *Nat. Methods 4* (3), 207−214.
(49) Park, S. K., Venable, J. D., Xu, T., and Yates, J. R. (2008) A quantitative analysis software tool for mass spectrometry−based proteomics. *Nat. Methods 5* (4), 319−322.
(50) Xia, J., Wishart, D. S., Xia, J., and Wishart, D. S. (2016) Using MetaboAnalyst 3.0 for Comprehensive Metabolomics Data Analysis, in *Current Protocols in Bioinformatics*, pp 14.10.1−14.10.91, John Wiley & Sons, Inc., Hoboken, NJ, DOI: 10.1002/cpbi.11.
(51) Benjamini, Y., and Hochberg, Y. (1995) Controlling the False Discovery Rate: A Practical and Powerful Approach to Multiple. *J. Royal Stat. Soc., Ser. B 57*, 289−300.
(52) Schneider, C. A., Rasband, W. S., and Eliceiri, K. W. (2012) NIH Image to ImageJ: 25 years of image analysis. *Nat. Methods 9* (7), 671−675.

DOI: 10.1021/acsinfecdis.8b00338
ACS Infect. Dis. 2019, 5, 851−862